



A high signal-to-noise Ca^{2+} probe composed of a single green fluorescent protein

Junichi Nakai*, Masamichi Ohkura, and Keiji Imoto

Department of Information Physiology, National Institute for Physiological Sciences, Myodaiji, Okazaki, 444-8585, Japan.

*Corresponding author (jnakai@nips.ac.jp).

Received 12 July 2000; accepted 20 November 2000

Recently, several groups have developed green fluorescent protein (GFP)-based Ca^{2+} probes. When applied in cells, however, these probes are difficult to use because of a low signal-to-noise ratio. Here we report the development of a high-affinity Ca^{2+} probe composed of a single GFP (named G-CaMP). G-CaMP showed an apparent K_d for Ca^{2+} of 235 nM. Association kinetics of Ca^{2+} binding were faster at higher Ca^{2+} concentrations, with time constants decreasing from 230 ms at 0.2 μM Ca^{2+} to 2.5 ms at 1 μM Ca^{2+} . Dissociation kinetics ($\tau \sim 200$ ms) are independent of Ca^{2+} concentrations. In HEK-293 cells and mouse myotubes expressing G-CaMP, large fluorescent changes were observed in response to application of drugs or electrical stimulations. G-CaMP will be a useful tool for visualizing intracellular Ca^{2+} in living cells. Mutational analysis, together with previous structural information, suggests the residues that may alter the fluorescence of GFP.

Keywords: calcium, green fluorescent protein, calmodulin, myosin light chain kinase, protein-protein interaction, photoisomerization

The measurement of intracellular Ca^{2+} concentration, $[\text{Ca}^{2+}]_i$, became practical and common after chemically synthesized Ca^{2+} indicators were developed. However, these indicators have significant limitations. For example, although these indicators are loaded into cells as acetoxymethyl esters, such loading does not enable targeting to specific cells. A means of Ca^{2+} measurement that allows genetic targeting to specific cells is the use of aequorin¹, a Ca^{2+} -sensitive chemiluminescent protein. However, aequorin requires coelenterazine, a chemical cofactor that is consumed during the production of luminescence.

The limitations of both aequorin and chemically synthesized indicators do not exist for the recently developed Ca^{2+} probes based on GFP (ref. 2). Ca^{2+} probes using fluorescence resonance energy transfer (FRET) (cameleon^{3,4} and FIP-CB_{SM}, refs 5, 6) were developed first, followed by the later development of a probe that uses conformational changes of GFP itself (camgaroo1⁷). Recently, yet another type of probe, which uses chemiluminescence resonance energy transfer, has been developed⁸. Although several reports using these Ca^{2+} probes have already been published⁹⁻¹⁶, limited signal intensity of the probes has made it difficult to measure $[\text{Ca}^{2+}]_i$ with good spatial and temporal resolution.

Here we have developed a Ca^{2+} probe based on a single GFP molecule with high Ca^{2+} affinity (named G-CaMP). We identified a residue (148) that has a significant impact of the fluorescent properties of the probe and predicted additional sites of the fusion protein that may have important effects on GFP fluorescence.

Results and discussion

Structure of Ca^{2+} probes. We designed Ca^{2+} probes containing either an enhanced GFP (EGFP) or a circularly permuted EGFP (cpEGFP), because this type of probe⁷ gives much greater fluores-

cent changes than FRET-based Ca^{2+} probes³⁻⁶. Because cpEGFP-based probes produced larger fluorescent changes than EGFP-based probes, we report here cpEGFP-based Ca^{2+} probes. The N terminus of cpEGFP was connected to the M13 fragment of myosin light chain kinase (M13; refs 5, 17), which is a target sequence of calmodulin (CaM; ref. 18), whereas the C terminus of cpEGFP was connected to CaM (Fig. 1A, B). When Ca^{2+} binds to CaM, conformational changes due to the Ca^{2+} -CaM-M13 interaction induce a subsequent conformational change in cpEGFP, so that the fluorescence intensity changes. We also made a Ca^{2+} probe that had CaM at the N terminus and M13 at the C terminus of cpEGFP, but it showed only small responses to Ca^{2+} (data not shown).

Screening of Ca^{2+} probes in HEK cells. First, we tested various cpEGFPs, in which the N terminus starts at amino acid residues 145 to 155 and the C terminus ends at residues 142 to 148, according to previously published work⁷. We transiently expressed the Ca^{2+} probes in HEK-293 cells, because application of ATP or carbachol induces Ca^{2+} release from intracellular Ca^{2+} stores¹⁹.

In agreement with the previous work⁷, the folding of cpEGFPs was temperature-sensitive such that the cpEGFPs became fluorescent at 28°C, but not at 37°C. Confocal imaging showed that the probes were expressed in the cytosol (Fig. 2A). Of all the cpEGFPs tested, two clones, G3 (which has cpEGFP149-144, where the numbers indicate amino acid residues at the N and C termini of cpEGFP, respectively) and G22 (which has cpEGFP150-144), produced acceptable responses to Ca^{2+} (Figs 1A, 2B, Table 1). The agonist-induced responses often had initial spikes followed by a sustained plateau (Fig. 2B) and were occasionally accompanied by a fluorescent oscillation with a frequency of ~ 0.1 Hz (data not shown). The ATP response of G3 ($\Delta F/F$ of 0.6) was slightly smaller than the carbachol response ($\Delta F/F$ of 0.8; $n = 15$). The fluores-





RESEARCH ARTICLES

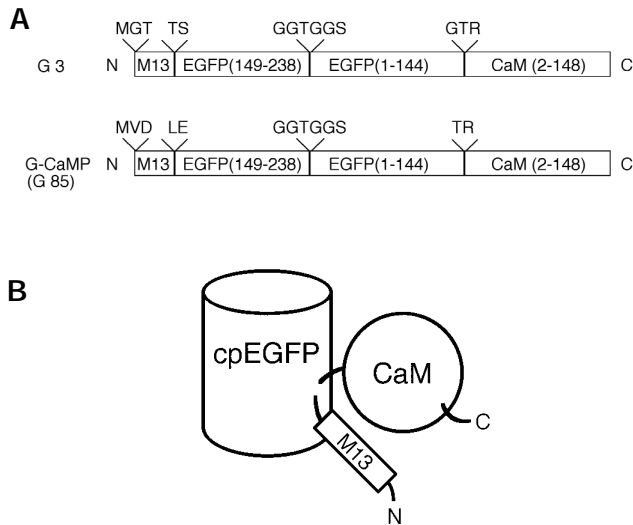


Figure 1. Schematic representation of GFP-based Ca^{2+} probes. **(A)** All Ca^{2+} probes consist of the M13 fragment from myosin light chain kinase (M13), a circularly permuted EGFP (cpEGFP) and calmodulin (CaM) located N to C terminally. The start- and end-residue numbers are shown in parentheses. Linkers are indicated above the structures in one-letter amino acid code. **(B)** Schematic topology of GFP-based Ca^{2+} probes.

cence increase in response to ATP was similar for G3 and G22 (Table 1).

G3 and G22 showed a marked fluorescence decrease at the beginning of excitation (Fig. 2B). Subsequently, both Ca^{2+} probes recovered fluorescence after several tens of seconds in the dark, indicating that the fluorescence decrease results from photoisomerization, but not from bleaching. This photoisomerization, however, did not occur for a number of other cpEGFPs that we tested (data not shown). Comparison of amino acid sequences of these other cpEGFPs with those of G3 and G22 indicated that residue 148 might be responsible for the photoisomerization. To test this hypothesis, the connecting amino acid sequence between M13 and cpEGFP149–144 of G3, which contained residue 148, was changed to other amino acids (Table 1). Analysis of these mutants confirmed the hypothesis that when residue 148 has a hydroxyl side chain (G3, G17, G22, G47, and G77), the probes exhibit photoisomerization. Because crystallographic analysis has shown that the side chain of residue 148 projects toward the interior of the GFP β -barrel and interacts with the fluorophore²⁰, hydrogen bonding between the hydroxyl side chains of residue 148 and Tyr66, which is a component of the fluorophore, may be responsible for the photoisomerization. The photoisomerization we observed might relate to the on/off blinking of GFPs reported previously²¹.

From our results and the earlier crystallographic study²⁰, we can predict that other residues (Gln94, Arg96, and Glu222) may also interact with the fluorophore and modify GFP fluorescence intensity.

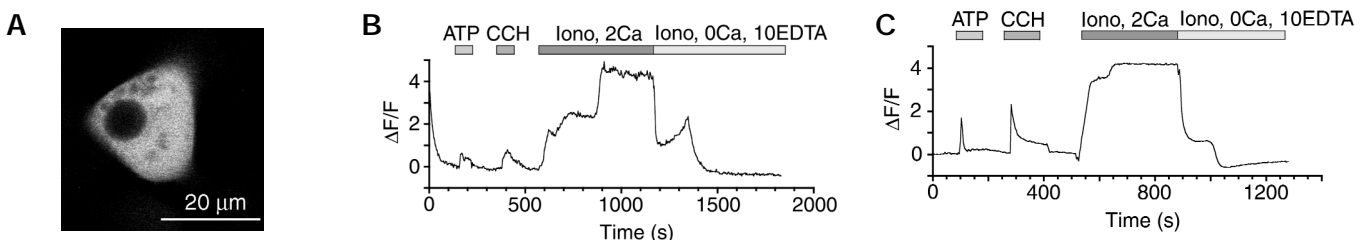


Figure 2. Expression of GFP-based Ca^{2+} probes in HEK-293 cells. **(A)** HEK-293 cell expressing cytosolic G3. **(B, C)** Fluorescent changes in response to drugs for cells expressing G3 **(B)** and G-CaMP **(C)**. Applications of 100 μM ATP, 100 μM carbachol (CCH), or 10 μM ionomycin (Iono) with and without Ca^{2+} are indicated by shaded bars.

Examination of residue 148 also gave us some information about the responsiveness to Ca^{2+} (Table 1). Whereas acidic side chains (aspartic acid in G52, glutamic acid in G18 and G79), and hydroxyl side chains (serine in G3 and G17, threonine in G22, tyrosine in G47) were acceptable for function, basic side chains (lysine in G62, arginine in G19 and G75) abolished responsiveness to Ca^{2+} . We also found that residue 147 is important. For example, G3 response to ATP was about two times stronger than that of G17, although G3 and G17 differ only at position 147 (threonine in G3, glycine in G17). Among the Ca^{2+} probes so far tested, G18 produced the best ATP responses (Table 1).

For further tuning of G18, we examined the effect of deleting glycine in the connecting sequence between cpEGFP and CaM (G72 and G85). G72 and G85, which were identical except for the N-terminal sequences, showed Ca^{2+} responsiveness similar to that of G18 (Table 1), but G72 and G85 were much brighter than G18 (data not shown). Because brighter probes are preferable to identify expressing cells, we chose G85 (hereafter named G-CaMP) for further characterization.

Responses of G-CaMP to agonists are shown in Figure 2C. In comparison with G3 (Fig. 2B), G-CaMP exhibited no photoisomerization and responded to agonists about three times better than G3. The responses of G-CaMP were also faster than those of G3, because initial spikes recorded from G-CaMP were sharper than those of G3. Intracellular pH (pHi) was also measured (data not shown), because G-CaMP is sensitive to pH (see below). During the application of ATP or carbachol, there was no change in pHi (pHi 7.3), indicating that fluorescent changes responded not to pHi but to $[\text{Ca}^{2+}]_i$. In the presence of 2 mM extracellular Ca^{2+} , the addition of ionomycin increased both $[\text{Ca}^{2+}]_i$ (as seen by an increase in fluorescence) and pHi (from 7.3 to 8.0). The addition of ionomycin plus ethylenediamine tetraacetic acid (EDTA) in the absence of extracellular Ca^{2+} resulted in a marked decrease in both $[\text{Ca}^{2+}]_i$ and pHi (which dropped from 8.0 to 7.0). After correction for the effects of pH, there was a 4.3-fold difference between maximum and minimum fluorescence. We estimated resting $[\text{Ca}^{2+}]_i$ to be between at 50 and 100 nM, and peak $[\text{Ca}^{2+}]_i$ during ATP application at ~ 250 nM, in good agreement with previous studies²².

In vitro characterization of the G-CaMP. Figure 3A shows fluorescence excitation and emission spectra of G-CaMP purified from bacteria. Excitation and emission maxima were 489 nm and 509 nm, respectively, similar to those of EGFP²³. Addition of Ca^{2+} increased fluorescence up to ~ 4.5 -fold. It is known that GFP forms homodimers at high protein concentrations. Gel filtration experiments at high (54.3 μM) and low (5.4 μM) protein concentrations revealed no shift in apparent molecular weight as a function of protein concentration, suggesting that G-CaMP exists as a monomer.

Figure 3B shows the Ca^{2+} titration of G-CaMP, which was fitted with a monophasic curve yielding an apparent K_d for Ca^{2+} of 235 nM and a Hill coefficient of 3.3 (at 0.3 μM protein concentration). The apparent K_d value was ~ 30 times lower than that of camgaroo1 (7 μM ; ref. 7). To determine whether the Ca^{2+} -CaM-M13 interaction

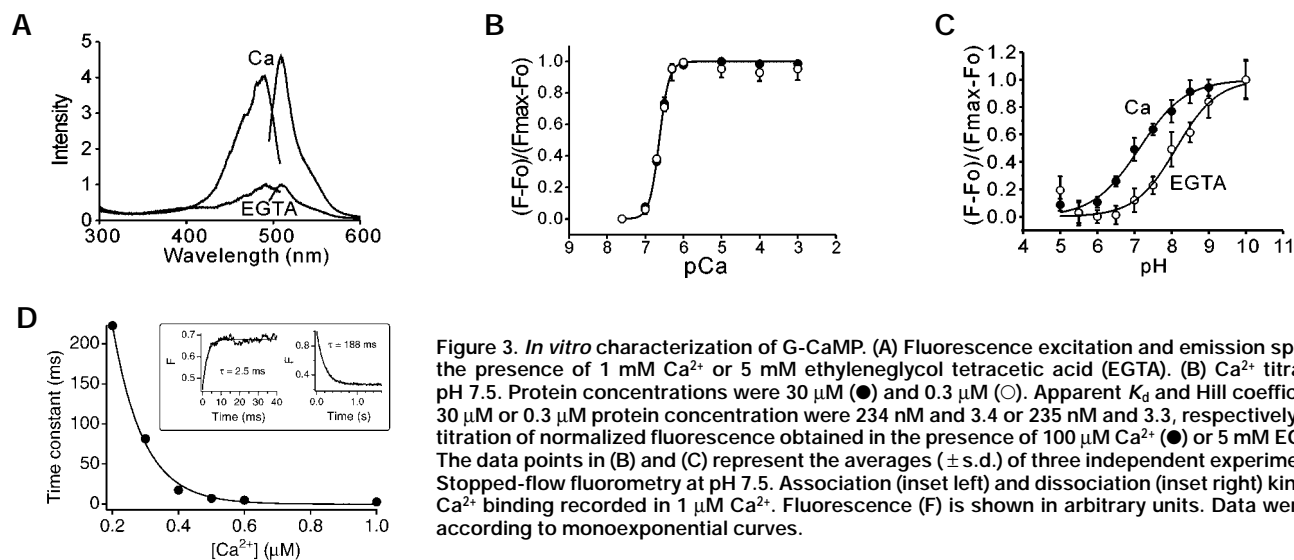


Figure 3. *In vitro* characterization of G-CaMP. (A) Fluorescence excitation and emission spectra in the presence of 1 mM Ca^{2+} or 5 mM ethyleneglycol tetracetic acid (EGTA). (B) Ca^{2+} titration at pH 7.5. Protein concentrations were 30 μM (●) and 0.3 μM (○). Apparent K_d and Hill coefficient for 30 μM or 0.3 μM protein concentration were 234 nM and 3.4 or 235 nM and 3.3, respectively. (C) pH titration of normalized fluorescence obtained in the presence of 100 μM Ca^{2+} (●) or 5 mM EGTA (○). The data points in (B) and (C) represent the averages (\pm s.d.) of three independent experiments. (D) Stopped-flow fluorometry at pH 7.5. Association (inset left) and dissociation (inset right) kinetics of Ca^{2+} binding recorded in 1 μM Ca^{2+} . Fluorescence (F) is shown in arbitrary units. Data were fitted according to monoexponential curves.

is intramolecular or intermolecular, Ca^{2+} titration was done at both low (0.3 μM) and high (30 μM) protein concentrations. Figure 3B revealed that there was no concentration-dependent difference in the apparent K_d of G-CaMP. In addition, gel filtration analysis revealed no shift in apparent molecular weight at 1 mM and zero Ca^{2+} concentrations. These results suggest that the Ca^{2+} -CaM-M13 interaction is intramolecular and that G-CaMP functions as a monomer.

Figure 3C illustrates the pH sensitivity of G-CaMP. Apparent p K_a values with and without Ca^{2+} were 7.1 and 8.1, respectively. Figure 3D shows the Ca^{2+} -binding kinetics of G-CaMP. The dissociation time constant ($\tau \sim 200$ ms) did not depend on $[\text{Ca}^{2+}]$ (only data at 1 μM are shown in Fig. 3D inset right), whereas the association

time constant is faster at increasing $[\text{Ca}^{2+}]$. Thus, these data indicate that association kinetics of G-CaMP are fast enough at high $[\text{Ca}^{2+}]$ ($\tau < 10$ ms for $[\text{Ca}^{2+}] > 500$ nM) to make the probe suitable for monitoring $[\text{Ca}^{2+}]_i$ in excitable cells.

Application of the Ca^{2+} probe to myotubes. We next tested G-CaMP in myotubes, in which $[\text{Ca}^{2+}]_i$ rises quickly upon depolarization. Figure 4A illustrates that electrical stimulation elicited a local depolarization-induced increase in $[\text{Ca}^{2+}]_i$ within a restricted region near the stimulating electrode (image 2), followed by a Ca^{2+} wave that propagated to an adjacent region (image 3). Carbachol and caffeine, which are known to increase $[\text{Ca}^{2+}]_i$ in myotubes, also induced substantial increases in fluorescence (Fig. 4B). pHi did not

Table 1. Identity and fluorescent responses for GFP-based Ca^{2+} probes^a

Probe number	N-terminal sequence	Sequence connecting M13 with cpEGFP	cpEGFP	Sequence connecting cpEGFP with CaM	ATP response ($\Delta F/F$)	n^b	Photoisomerization
G3	MGT	TS	149-144	GTR	0.7	28	+++
G17	MGT	GS	149-144	GTR	0.3	11	+++
G18	MGT	LE	149-144	GTR	1.6	78	-
G19	MGT	PR	149-144	GTR	0	12	-
G41	MGT	TI	149-144	GTR	0	18	-
G44	MGT	TP	149-144	GTR	0	21	-
G46	MGT	TA	149-144	GTR	0	12	-
G47	MGT	TY	149-144	GTR	0.7	19	++
G49	MGT	TQ	149-144	GTR	0	18	-
G50	MGT	TN	149-144	GTR	0	18	-
G52	MGT	TD	149-144	GTR	0.3	20	-
G54	MGT	TC	149-144	GTR	0.3	21	-
G55	MGT	TW	149-144	GTR	0	20	-
G56	MGT	TG	149-144	GTR	0	20	-
G58	MGT	TV	149-144	GTR	0	23	-
G61	MGT	TF	149-144	GTR	0.5	22	-
G62	MGT	TK	149-144	GTR	0	28	-
G72	MGT	LE	149-144	TR	1.6	67	-
G75	MVD	TR	149-144	GTR	0	29	-
G76	MVD	TM	149-144	GTR	0.6	23	-
G77	MVD	TT	149-144	GTR	0.1	10	+++
G79	MVD	TE	149-144	GTR	0.5	26	-
G80	MVD	TH	149-144	GTR	0.3	23	+
G81	MVD	TL	149-144	GTR	0.6	8	-
G85(G-CaMP)	MVD	LE	149-144	TR	1.5	16	-
G22	MGT	TS	150-144	GTR	0.6	26	+++

^aAmino acids are indicated using one-letter code. Residues 147 and 148 of cpEGFP149-144 and residue 148 (threonine) of cpEGFP150-144 are included in the linker sequences connecting M13 with cpEGFP.

^bNumber of cells tested.



RESEARCH ARTICLES

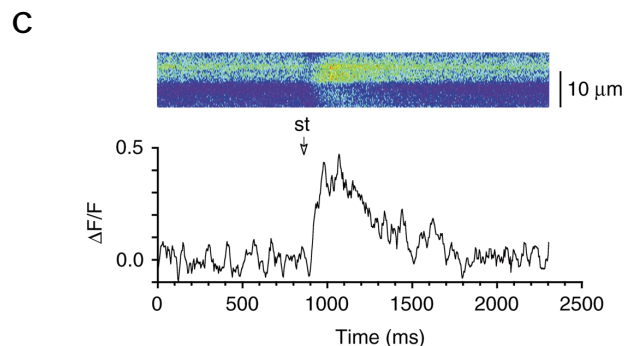
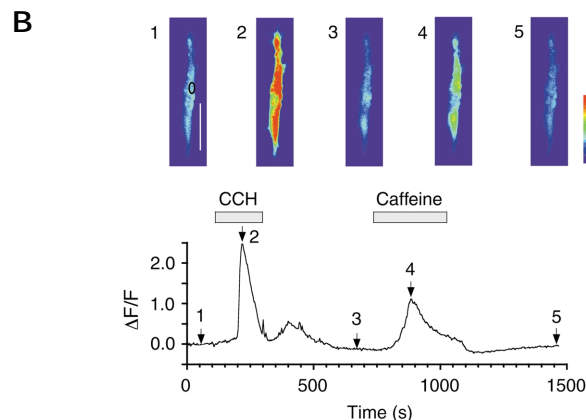
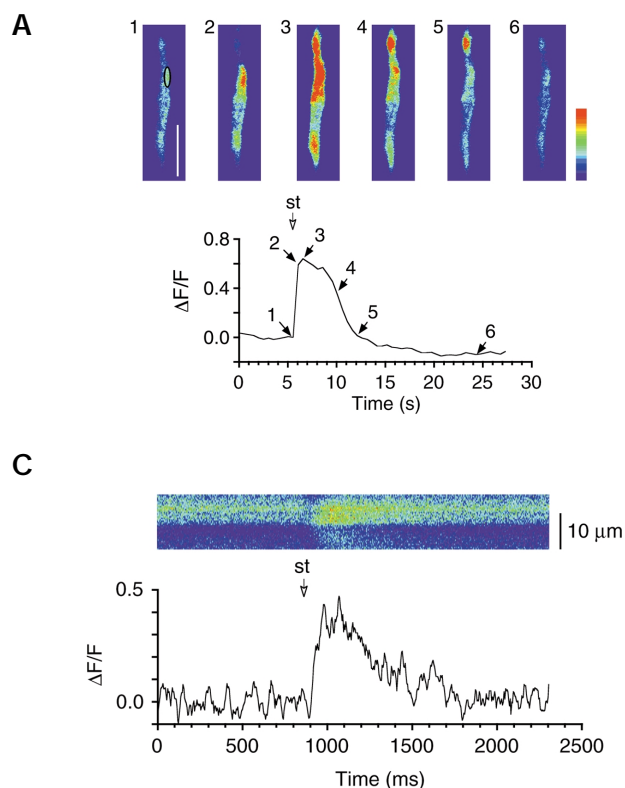


Figure 4. Expression of G-CaMP in myotubes. (A and B) Lower panels show the time course of fluorescent signal from a region indicated by a black oval in each image 1. Images were taken at the indicated time. Scale bars indicate 100 μm . (A) Extracellular electrical stimulation (st) induced an increase in $[\text{Ca}^{2+}]_i$. The stimulation electrode was placed in the right side of the middle portion of the cell. Interval time between frames was 0.5 s. (B) 100 μM carbachol (CCH) and 10 mM caffeine-induced increases in $[\text{Ca}^{2+}]_i$ monitored with G-CaMP. The relatively slow onset of the responses was due to the big chamber and slow perfusion rate of the system. (C) The upper panel shows a confocal line-scan image of depolarization-induced $[\text{Ca}^{2+}]_i$ increase. The lower panel shows the time course of the change in fluorescence of the above image. Extracellular electrical stimulation (st) was delivered at the indicated time.

change during the experiments (pHi 7.3; data not shown). The depolarization-induced increase in $[\text{Ca}^{2+}]_i$ was further analyzed by confocal line-scan imaging (Fig. 4C). The fluorescence increase showed an initial rapid phase and a subsequent slow phase of $[\text{Ca}^{2+}]_i$ increase, followed by recovery to the basal Ca^{2+} level. The rapid phase lasted ~ 60 ms and $[\text{Ca}^{2+}]_i$ reached its maximum within 200 ms. The time course of the fluorescence increase measured with G-CaMP is similar to that previously found in myotubes with Fluo 3 (ref. 24).

In the work described here, we developed a high signal-to-noise Ca^{2+} probe based on a single GFP protein (G-CaMP). The improved signal over background ratio due to the increased affinity is a major advantage of G-CaMP. Although G-CaMP exhibits pH sensitivity and the requirement of folding at temperatures below 37°C , Ca^{2+} responses are sufficiently large and fast that G-CaMP should prove to be a powerful tool in studies of Ca^{2+} dynamics in excitable cells. On the other hand, accurate measurements of micromolar $[\text{Ca}^{2+}]_i$ might best be achieved using camgaroo1 because of its moderate Ca^{2+} affinity and broad dynamic range⁷. By introducing the cDNA with specific promoters into animals and plants, expression of the probe could be controlled spatially and temporally.

Experimental protocol

Plasmid construction. The original circular permutation of EGFP (cpEGFP145–144) was made using pEGFP-N1 (Clontech, Palo Alto, CA) by PCR. Amplification of cpEGFP149–144 and cpEGFP150–144 from cpEGFP145–144 was by PCR, both of which had a *SpeI* site (encoding amino acid residues Thr-Ser) at the 5' end and GGG (encoding glycine) with a *MluI* site (Thr-Arg) at the 3' end. The complementary DNA (cDNA) encoding the chicken smooth muscle M13 (SSRRKWNKTGHAVRAIGRLSS; refs 5, 17), which was preceded by a *NheI* site, Kozak sequence (CGCCACC), start codon (ATG), and a *KpnI* site (Gly-Thr), was connected to cpEGFP149–144 at the *SpeI* site. The 3' end of cpEGFP149–144 was connected to the PCR fragment encoding amino acid residues 2–148 of rat calmodulin (pRCaM; ref. 18) at the *MluI* site. The calmodulin sequence was followed by a stop codon and a *NotI* site. The entire coding sequence was inserted into the *NheI* and *NotI* sites of pEGFP-N1 to yield pN1-G3. We used PCR to make pN1-

G17, 18, 19 or 21, and replaced the connecting sequence between M13 and cpEGFP149–144 of pN1-G3 (the *SpeI* site) by *BamHI* (Gly-Ser), *XhoI* (Leu-Glu), *SacII* (Pro-Arg), or *PvuI* (Arg-Ser) site, respectively (G21 did not produce fluorescence.) pN1-G22 includes cpEGFP150–144 instead of cpEGFP149–144. In pN1-G72, the GGG (glycine) sequence preceding the *MluI* site of pN1-G18 was deleted. For pN1-G75, 76, 77, 79, 80, 81, and 85, the *NheI* and *KpnI* sites before and after the start codon of pN1-G72 were substituted by *BglII* and *SalI* (Val-Asp) sites, respectively. Site-directed mutations were also done by PCR.

Bacterial expression and *in vitro* fluorescence measurements. The *NcoI-NotI* cDNA fragment of pN1-G85 was inserted into pET23d(+) or pET32a (Novagen, Madison, WI), resulting in pET23d-G85 or pET32a-G85, respectively. pET32a-G85 produced a construct that possessed a polyhistidine tag at the N terminus, whereas pET23d-G85 resulted in a nontagged construct. There was no difference in behavior with and without the tag.

Escherichia coli BL21 (DE3)pLysS transformed with the plasmids were cultured at 28°C for 4 h after protein induction with 1 mM isopropyl- β -D-thiogalactoside (IPTG). Cells were lysed by freezing (for 30 min at -20°C) and thawing (for 30 min at room temperature) three times and suspended with a solution of 25 mM Tris-HCl (pH 8), 1 mM β -mercaptoethanol, and protease inhibitors. After centrifugation the supernatant was dialyzed against KM buffer containing (in mM) 100 KCl and 20 MOPS (pH 7.5). A NiNTA resin (Qiagen, Hilden, Germany) was used for purification of the tagged protein. Gel filtration was performed using Sephadex G-100.

Excitation spectra (detected at 520 nm) and emission spectra (excited at 470 nm) were taken with the fluorescent spectrophotometer F4500 (Hitachi, Tokyo, Japan). For Ca^{2+} titration experiments, free Ca^{2+} concentrations with 20 mM BAPTA were calculated using MaxChelator program²⁵. The fluorescence excited at 480 nm was monitored at 510 nm. Data were fit according to the Hill equation. For pH titration experiments at 1.1 μM protein concentration, MOPS (for pH 6 to 8) in KM buffer was replaced with either citrate (for pH 5 to 6) or glycine (for pH 8 to 10). Stopped-flow fluorometry RSP-601 (Unisoku, Osaka, Japan) was done at 26°C . Fluorescence at pH 7.5 was excited at 488 nm and emission was detected at 510 nm. Concentrations quoted are those before 1:1 mixing. Mixing dead time was 1 ms. Data were averaged at least three times. For measurements of association kinetics, the purified protein (30 μM) in 2 mM BAPTA was mixed with various amount of Ca^{2+} . Identical results were obtained using 5 mM BAPTA (data not shown). For measurements of the dissociation kinetics, the purified protein (30 μM) in 1 mM BAPTA with 1, 10, or 50 μM free Ca^{2+} was mixed with 17 mM BAPTA.



Fluorescence measurements in HEK cells. HEK-293 cells were cultured and transfected with the plasmids as described²². Cells were incubated at 28°C for two to four days before testing. Fluorescence excited at 488 nm was detected at 525 ± 25 nm with a confocal laser scanning microscope (interval time 2 s). A solution containing (in mM) 135 NaCl, 5.4 KCl, 2 CaCl₂, 1 MgCl₂, 10 glucose, 5 HEPES (pH 7.4) or HEPES-buffered saline²² was used in the experiments.

We estimated the physiological pHi to be 7.3, with pHi 8.0 and pHi 7.0 corresponding to the maximum fluorescence (F_{max}) and minimum fluorescence (F_{min}), respectively, as described elsewhere²⁶. For estimation of $[Ca^{2+}]_i$, fluorescent signals were corrected for pHi using the pH titration curves in Figure 3C. pCa was subsequently calculated using the following equation: $pCa = 1/n \times \log[(F_{max,corr} - F) / (F - F_{min,corr})] - \log K_d$, where n is the Hill coefficient obtained from Figure 3B, $F_{max,corr}$ and $F_{min,corr}$ are the maximum and minimum fluorescence values corresponding to pH 7.3, respectively, F is the experimental fluorescence, and K_d is the apparent dissociation constant obtained from Figure 3B.

Fluorescence measurements in myotubes. Preparation of mouse myotubes (BALB/c) was as described²⁷. After introduction of cDNA into cells²⁷, they were cultured at 28°C for an additional two to four days before testing. Extracellular electrical stimulation was done as described²⁷. Fluorescent images were recorded with the confocal microscope. For line-scan images, a scan speed of 4.5 ms/line was used and the raw data were subsequently filtered using a box filter.

Acknowledgments

We thank Masayuki Mori for the rat calmodulin cDNA and Michiyo Murata and Mitsutoshi Ono for technical assistance. We also thank Toshihiko Nagamura and Tatsuo Nakagawa of Unisoku Co., Ltd. for technical assistance. The work was supported by grants from the Ministry of Education, Science, Sports and Culture, by "the Research for the Future Program" of the JSPS, and by the JSPS Research Fellowships for Young Scientists.

- Inouye, S. *et al.* Cloning and sequence analysis of cDNA for the luminescent protein aequorin. *Proc. Natl. Acad. Sci. USA* **82**, 3154–3158 (1985).
- Prasher, D.C., Eckenrode, V.K., Ward, W.W., Prendergast, F.G. & Cormier, M.J. Primary structure of the *Aequorea victoria* green-fluorescent protein. *Gene* **111**, 229–233 (1992).
- Miyawaki, A. *et al.* Fluorescent indicators for Ca²⁺ based on green fluorescent proteins and calmodulin. *Nature* **388**, 882–887 (1997).
- Miyawaki, A., Griesbeck, O., Heim, R. & Tsien, R.Y. Dynamic and quantitative Ca²⁺ measurements using improved cameleons. *Proc. Natl. Acad. Sci. USA* **96**, 2135–2140 (1999).
- Romoser, V.A., Hinkle, P.M. & Persechini, A. Detection in living cells of Ca²⁺-dependent changes in the fluorescence emission of an indicator composed of two green fluorescent protein variants linked by a calmodulin-binding sequence. A new class of fluorescent indicators. *J. Biol. Chem.* **272**, 13270–13274 (1997).

- Persechini, A., Lynch, J.A. & Romoser, V.A. Novel fluorescent indicator proteins for monitoring free intracellular Ca²⁺. *Cell Calcium* **22**, 209–216 (1997).
- Baird, G.S., Zacharias, D.A. & Tsien, R.Y. Circular permutation and receptor insertion within green fluorescent proteins. *Proc. Natl. Acad. Sci. USA* **96**, 11241–11246 (1999).
- Baubet, V. *et al.* Chimeric green fluorescent protein–aequorin as bioluminescent Ca²⁺ reporters at the single-cell level. *Proc. Natl. Acad. Sci. USA* **97**, 7260–7265 (2000).
- Allen, G.J. *et al.* Cameleon calcium indicator reports cytoplasmic calcium dynamics in *Arabidopsis* guard cells. *Plant J.* **19**, 735–747 (1999).
- Emmanouilidou, E. *et al.* Imaging Ca²⁺ concentration changes at the secretory vesicle surface with a recombinant targeted cameleon. *Curr. Biol.* **9**, 915–918 (1999).
- Fan, G.Y. *et al.* Video-rate scanning two-photon excitation fluorescence microscopy and ratio imaging with cameleons. *Biophys. J.* **76**, 2412–2420 (1999).
- Jacobi, M. *et al.* Inositol 1,4,5-trisphosphate directs Ca²⁺ flow between mitochondria and the endoplasmic/sarcoplasmic reticulum: a role in regulating cardiac autonomic Ca²⁺ spiking. *Mol. Biol. Cell* **11**, 1845–1858 (2000).
- Foyouzi-Youssefi, R. *et al.* Bcl-2 decreases the free Ca²⁺ concentration within the endoplasmic reticulum. *Proc. Natl. Acad. Sci. USA* **97**, 5723–5728 (2000).
- Yu, R. & Hinkle, P.M. Rapid turnover of calcium in the endoplasmic reticulum during signaling: studies with cameleon calcium indicators. *J. Biol. Chem.* **275**, 23648–23653 (2000).
- Kerr, R. *et al.* Optical imaging of calcium transients in neurons and pharyngeal muscle of *C. elegans*. *Neuron* **26**, 583–594 (2000).
- Allen, G.J. *et al.* Alteration of stimulus-specific guard cell calcium oscillations and stomatal closing in *Arabidopsis det3* mutant. *Science* **289**, 2338–2342 (2000).
- Rhoads, A.R. & Friedberg, F. Sequence motifs for calmodulin recognition. *FASEB J.* **11**, 331–340 (1997).
- Mori, M. *et al.* Novel interaction of the voltage-dependent sodium channel (VDSC) with calmodulin: does VDSC acquire calmodulin-mediated Ca²⁺-sensitivity? *Biochemistry* **39**, 1316–1323 (2000).
- Bischof, G., Serwold, T.F. & Machen, T.E. Does nitric oxide regulate capacitative Ca influx in HEK 293 cells? *Cell Calcium* **21**, 135–142 (1997).
- Yang, F., Moss, L.G. & Phillips, G.N. Jr. The molecular structure of green fluorescent protein. *Nat. Biotechnol.* **14**, 1246–1251 (1996).
- Dickson, R.M., Cubitt, A.B., Tsien, R.Y. & Moerner, W.E. On/off blinking and switching behavior of single molecules of green fluorescent protein. *Nature* **388**, 355–358 (1997).
- Okada, T. *et al.* Molecular and functional characterization of a novel mouse transient receptor potential protein homologue TRP7. *J. Biol. Chem.* **274**, 27359–27370 (1999).
- Cormack, B.P., Valdivia, R.H. & Falkow, S. FACS-optimized mutants of the green fluorescent protein (GFP). *Gene* **173**, 33–38 (1996).
- Nakai, J. *et al.* Functional nonequality of the cardiac and skeletal ryanodine receptors. *Proc. Natl. Acad. Sci. USA* **94**, 1019–1022 (1997).
- Bers, D.M., Patton, C.W. & Nuccitelli, R. A practical guide to the preparation of Ca²⁺ buffers. *Methods Cell Biol.* **40**, 3–29 (1994).
- James-Krache, M.R. Quick and accurate method to convert BCECF fluorescence to pHi: calibration in three different types of cell preparations. *J. Cell. Physiol.* **151**, 596–603 (1992).
- Tanabe, T., Beam, K.G., Powell, J.A. & Numa, S. Restoration of excitation–contraction coupling and slow calcium current in dysgenic muscle by dihydropyridine receptor complementary DNA. *Nature* **336**, 134–139 (1988).